Biophysical Journal, Volume *114*

Supplemental Information

Molecular Dynamics Analysis of Cardiolipin and Monolysocardiolipin on Bilayer Properties

Kevin J. Boyd, Nathan N. Alder, and Eric R. May

Characterization of molecular and bilayer scale properties of cardiolipin and monolysocardiolipin from multi-scale molecular dynamics simulations

Kevin .J. Boyd, Nathan N. Alder, Eric R. May

Supplementary Methods

Electrostatics in GROMACS-LS

The current implementation of GROMACS-LS[1] does not support PME electrostatics to calculate the electrostatic forces component of the virial. The electrostatic force in GROMACS-LS must be calculated using a cutoff treatment for electrostatics, with the cutoff length extended beyond the typical short-range cutoff used for the direct space electrostatic calculation when using PME. It has been demonstrated that a cutoff of r_{ES} = 2.2 nm is sufficient for convergence of the LPP for a neutral lipid membrane, and is the recommended parameter choice of r_{ES} in GROMACS-LS.[1] However, the cardiolipin bilayer systems are highly charged and we were concerned that the electrostatic component of the virial may not be adequately calculated with r_{ES} =2.2 nm and may require a longer cutoff. We scanned a range of r_{ES} values for the TOCL membrane, we found that the profiles appear converged at a cutoff of 2.4 nm, **Fig S1.**

However, while the shape of the TOCL LPP is converged at r_{ES} = 2.4 nm, several key observables of the system continue to change as r_{ES} is increased. The average lateral and normal system pressures continue to change beyond the 2.4 nm cutoff. If the electrostatic treatment in the analysis (with a straight cutoff) is closely approximating the forces calculated during the production run (treated with PME), then the calculated total

lateral pressure (P_L =[P_{xx} + P_{yy}] / 2) and normal pressure (P_N = P_{zz}) from the analysis should match the pressures from the simulation run, which are being coupled to a pressure bath at 1 bar. **Fig S2** presents the calculated bulk lateral and normal pressures over a range of cutoffs. At short cutoffs, P_L is overestimated, which was also observed by Vanegas et al. in a POPE bilayer.[1] At a cutoffs of 2.6 nm and above, P_L approaches the correct bulk pressure (1 bar) but fluctuates in the range of +10 bar to -10 bar. P_N is slightly underestimated at low cutoffs and converges to the correct simulation pressure, within error estimate, at a cutoff of 3.0 nm.

The treatment of cutoffs in GROMACS-LS should be even more stringently considered when estimating elastic parameters from the LPP. We calculated the first moment of the LPP which is equal to the product of the bending modulus (k_c) times the spontaneous curvature (c_0) for TOCL over a range of electrostatic cutoffs (**Fig S3**), and found that the observed value of $k_c c_0$ decreased roughly linearly from a cutoff of 1.6 nm to 2.6 nm. The calculated values of $k_c c_0$ in the cutoff range of 2.8 nm to 3.2 nm were more similar to each other, indicating that the value was approaching convergence with respect to the cutoff length, but was still slowly decreasing. We note that the sign of $k_c c_0$ was only negative at the highest cutoff (3.2 nm). The sign of c_0 is inferred from the sign of $k_c c_o$; therefore, it is essential to check the convergence of the first moment of the LPP when attemptimg to estimate the sign of spontaneous curvature.

The dependence of system observables on electrostatic cutoff length in our system cannot necessarily be generalized to all lipid systems, as our TOCL and MLCL bilayers have a highly negative surface charge and required an high concentration of

sodium ions to balance the total system charge. A zwitterionic lipid bilayer with typical counterion concentrations may show converged properties at a lower cutoff, which would be advantageous as the computational requirements for calculating electrostatics with a straight cutoff scales cubically with distance. However, we suggest that for any analysis beyond simply observing the shape of the LPP, it is necessary to test the effect of electrostatic cutoffs on the parameter of interest.

Supplementary Figures

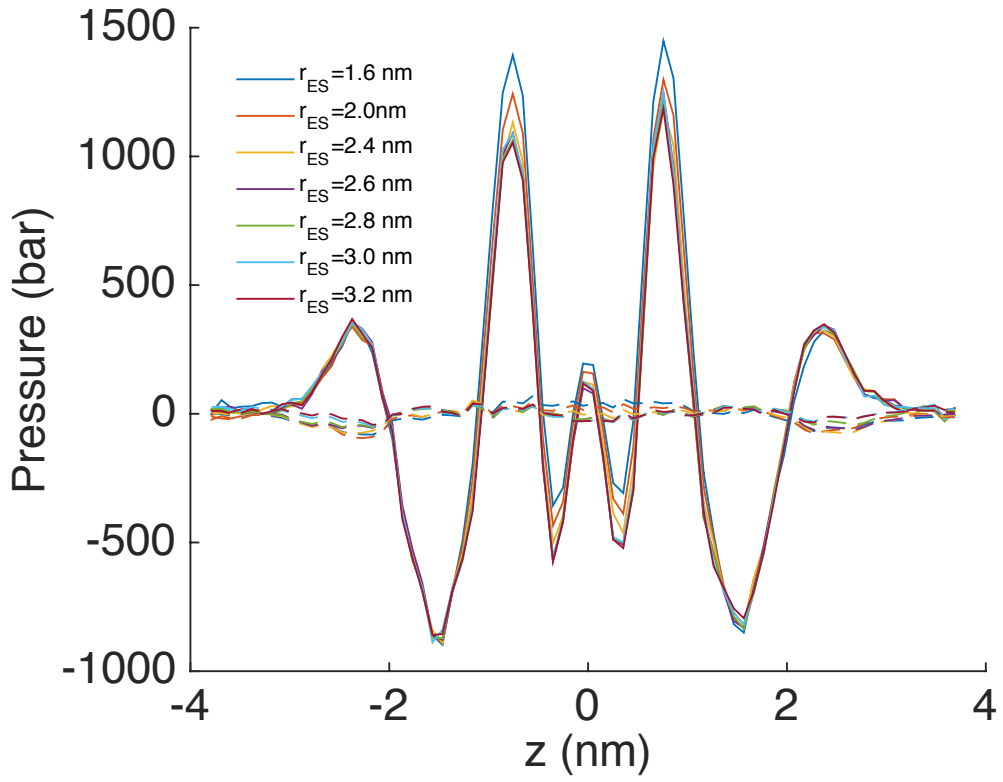

Fig S1. Pressure profile for a TOCL bilayer calculated for a range of electrostatic cutoff distances. Both the lateral (solid) and normal (dashed) components of the pressure profile are shown.

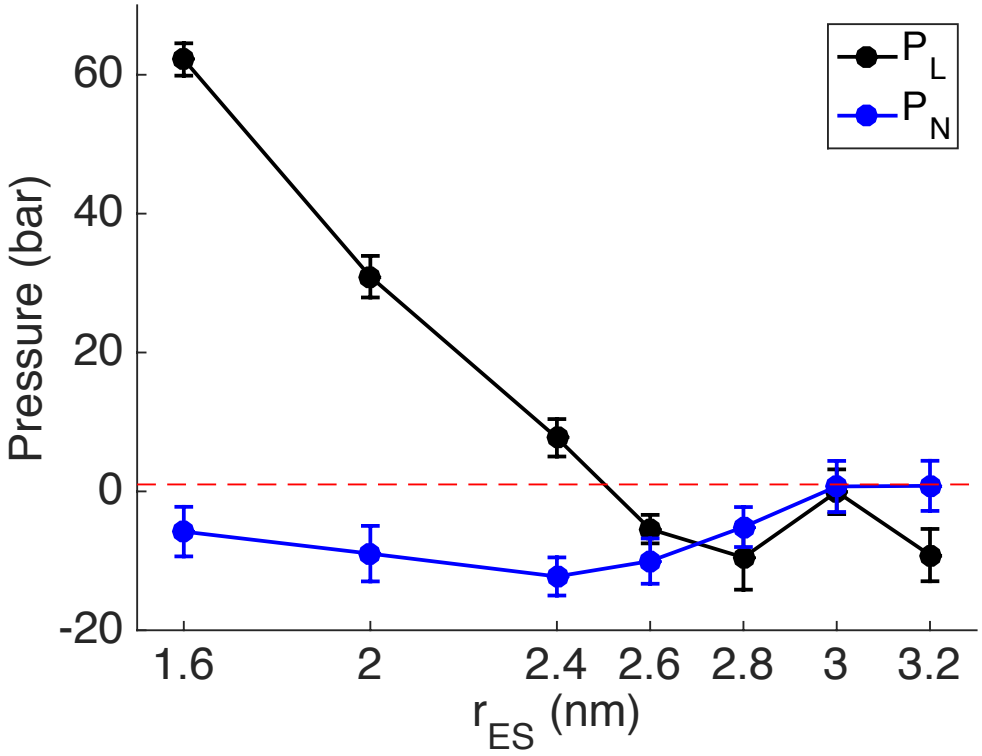

Fig S2. System pressures from GROMACS-LS. The lateral and normal components of the total system pressure for the TOCL bilayer were calculated over a range of electrostatic cutoffs by integrating $P_L(z)$ and $P_N(z)$ over the *z* dimension of the simulation box and dividing by the *z* dimension of the box. Dashed red line is drawn at 1 bar.

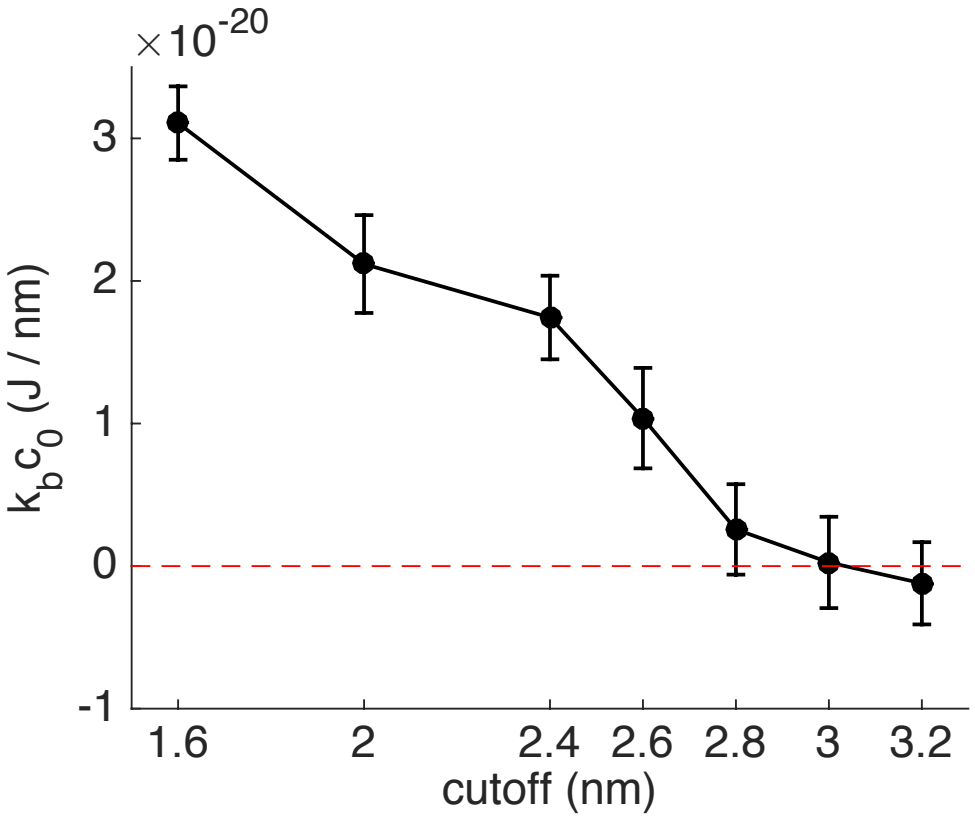

Fig S3. Effect of electrostatic cutoffs on $k_c c_o$. The first moment of the LPP of the TOCL bilayer ($k_c c_o$) was calculated over a range of electrostatic cutoffs. Error bars are standard errors of the mean. Dashed red line is drawn at $k_c c_0 = 0$

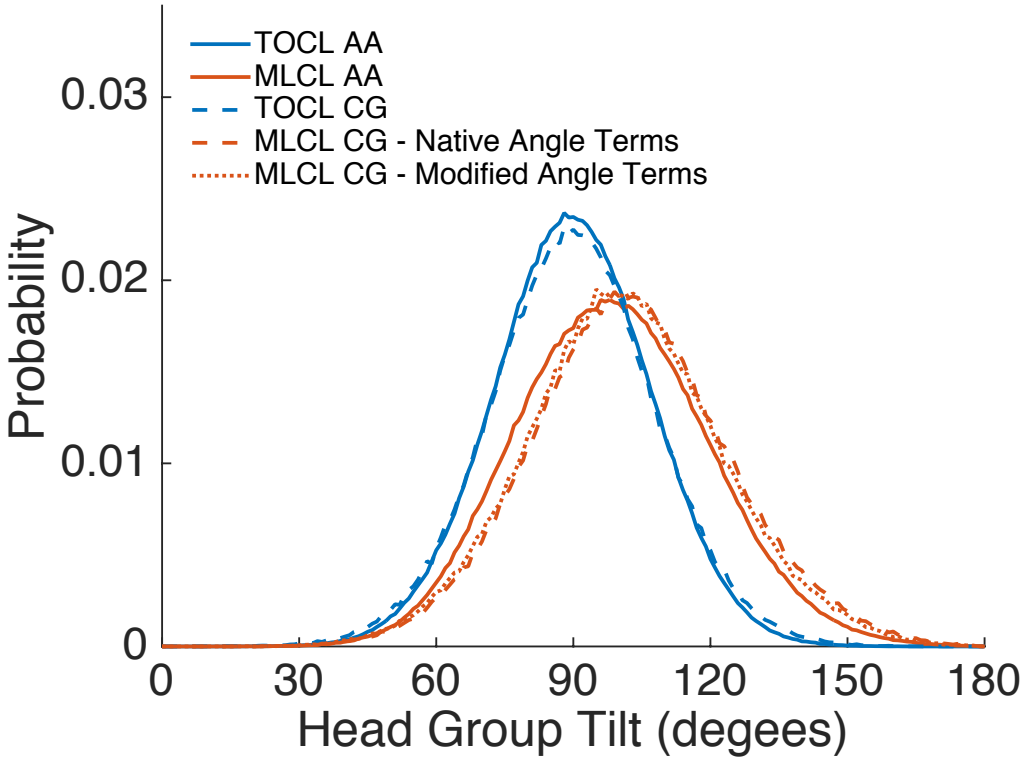

Fig S4. Comparison of headgroup tilting between atomistic and CG models. TOCL and MLCL tilting is compared between homogeneous bilayers using the CHARMM36 force field (AA) and Martini force field (CG). For the Martini MLCL the lyso side PGG angle term was removed (modified), but it showed no effect compared to when the PGG term was retained (native).

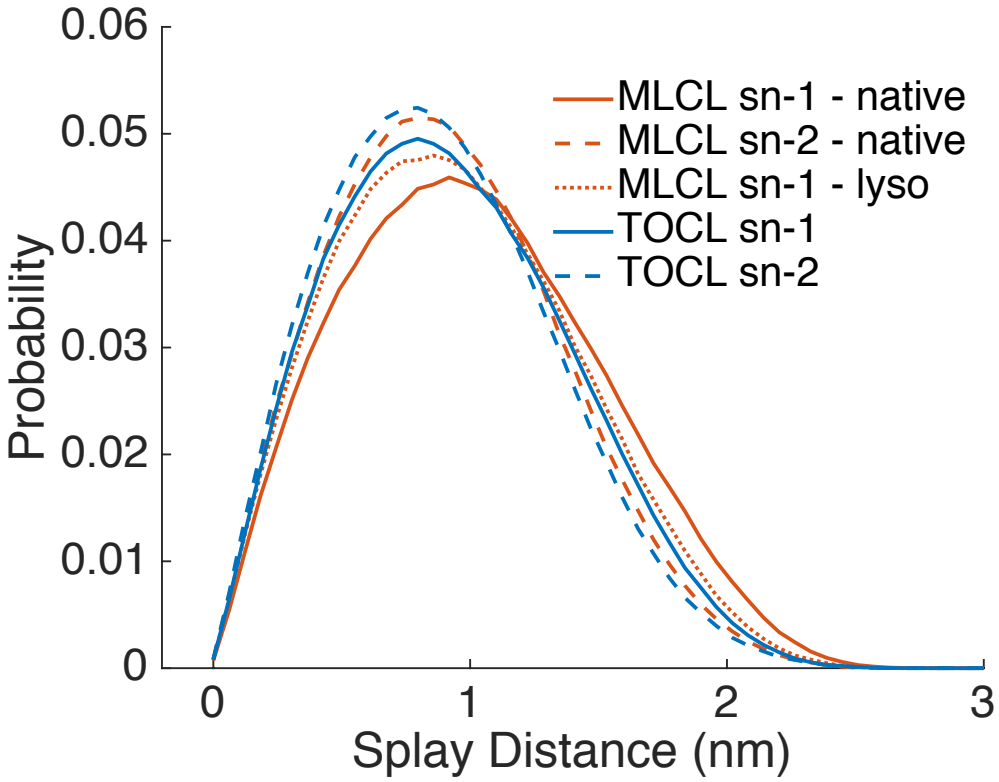

Fig S5. Acyl chain splay distances. The splay distances were calculated by projecting the vector connecting the central glycerol carbon to the terminal acyl chain carbon onto the *x-y* plane.

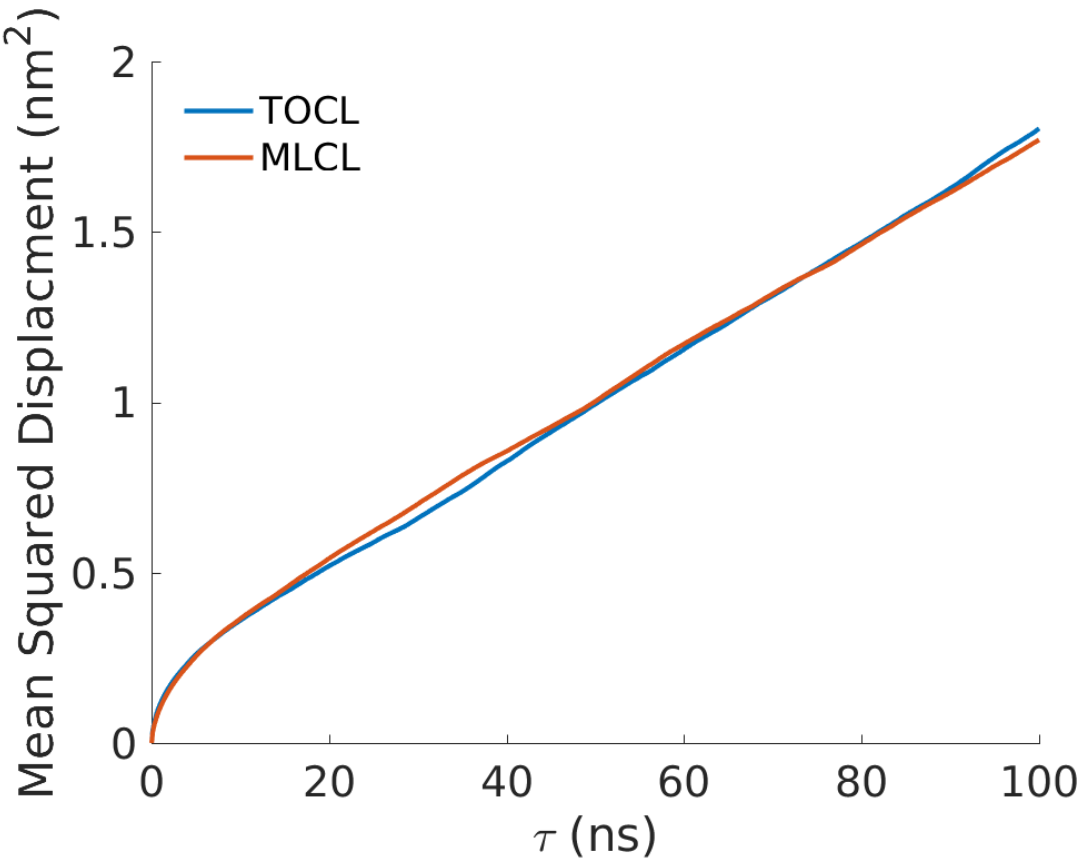

Fig S6. Lateral diffusion of atomistic TOCL and MLCL bilayers. Lateral mean squared displacements at a range of time lags (τ values) were calculated using gmx msd. Diffusion coefficients were extracted from a linear fit of the data ranging from τ=20 ns to τ=100 ns.

Supplementary Files

S1-S2 Files. Topology files for all-atom and CG MLCL

GROMACS compatible topology (.itp) files are included for MLCL, consistent with the all-atom CHARMM36 force field (**S1**) and the CG Martini force field (**S2**).

Supplementary References

1. Vanegas JM, Torres-Sánchez A, Arroyo M. Importance of force decomposition for local stress calculations in biomembrane molecular simulations. *J Chem Theory Comput*. 2014;10(2):691-702. doi:10.1021/ct4008926.